

CHAPTER VI
COMBINED CARBON DIOXIDE AND STEAM
REFORMING WITH METHANE IN LOW TEMPERATURE PLASMAS

6.1 Abstract

The combination of carbon dioxide reforming and steam reforming with methane was investigated in a corona discharge reactor with moderate power consumption. The plasma was used to overcome the energy barrier of these two endothermic reactions instead of high temperature catalytic processes. Simultaneous carbon dioxide and steam reforming produced higher methane conversions and CO/C₂ ratios than only steam reforming or carbon dioxide reforming. The H₂/CO ratio of 1.9:1 is close to that desired for Fischer Tropsch or methanol synthesis was achieved at a CO₂/CH₄ ratio of 1:1 with 50% water-vapor in the feed stream. In this condition, the energy consumption was about 12 eV/molecule of carbon converted. Using electricity to drive the reaction at low temperature is counter-balanced by lower costs and simpler operation.

6.2 Introduction

With increasing population and rapid technology development, we have been facing alteration of the climate. Greenhouse gases that include carbon dioxide, methane, ozone, halocarbons and nitrous oxide, to significant extents come from the combustion of fossil fuels (coal, oil, and natural gas) for power generation and transportation. A potentially useful reaction for reducing the impact of carbon dioxide (reducing net emissions), a major component in many natural gas resources, especially in Asia, is carbon dioxide reforming with methane (Reaction 6.1) for production of synthesis gas (carbon monoxide and hydrogen) at a lower H₂/CO ratio compared to steam reforming of methane (Reaction 6.2), which is a major conventional process for synthesis gas production. A typical industrial steam reformer operates at 1,120-1,170 K and 15-30 atm over a Ni/Al₂O₃ catalyst (1). However, as with steam reforming, the highly endothermic reaction requires

significant high temperature energy input that is usually provided by combustion that releases carbon dioxide. Also, the 1:1 H₂/CO ratio produced from carbon dioxide reforming requires, for GTL applications, the use of the water gas shift reaction, in which much of the potential net consumption of carbon dioxide is lost. However, a major problem with carbon dioxide reforming to this point in time is the deactivation of the catalyst due to carbon deposition (Reactions 6.3 and 6.4) at the desired reaction conditions.



So far, There is no any effective commercial catalyst which can operate without carbon formation (2). One of possible alternatives is to combine carbon dioxide reforming with steam reforming. A thermodynamics study has shown that the presence of water in carbon dioxide reforming allows increased methane conversion (3) and probably decreased carbon formation at a specific CO₂/CH₄ ratio. Moreover, for several feed ratios of CH₄/CO₂, the desired H₂/CO ratio at equilibrium is controllable by the amount of water added in feed stream, for example, the desired ratio of H₂/CO of 1:1 can be obtained from a Terrell natural gas by using up to 3.28% of water in the feed (3). Both carbon dioxide reforming and steam reforming have similar low net carbon dioxide reduction due to combustion needed to provide the required heat of reaction. Thus any net reduction of carbon dioxide impact from the process must be compared with partial oxidation or combined/autothermal reforming which is exothermic or self heating, but require the production of oxygen that is itself energy intensive. Therefore, rather than considering the net carbon dioxide reduction as the driver, other factors must be considered. For example, high carbon dioxide in natural gas resources may be stranded by the high cost of carbon dioxide removal, which may be reduced or eliminated by use of carbon dioxide reforming. Additionally, the possible lower capital investment and operating costs

due to the elimination of the requirement for oxygen makes consideration of this technology worthwhile. Due to the fact that both carbon dioxide reforming and steam reforming are endothermic reactions, the high reaction temperature requires an intensive energy input and a high operating cost. One may use non-equilibrium plasma to reduce energy cost instead of thermal process.

The non-thermal, also called cold plasma, with its non-equilibrium properties, high electron temperature and low bulk gas temperature, provides the capability for initiating chemical reactions at low temperatures and potentially with low energy input. The non-equilibrium plasma is used to overcome the energy barrier to start the reaction by promoting radical production (4).

Corona discharge and dielectric barrier discharge (DBD) techniques are two of the commonly used methods for producing non-equilibrium plasmas at atmospheric pressure (5). The utilization of the non-equilibrium plasma techniques for carbon dioxide reforming with methane has been studied in the dielectric barrier discharge (2, 6-8).

The spectroscopic characteristic of a plasma created in a methane and carbon dioxide mixture by a high-voltage, steep front-voltage, very-short-pulse triggered dielectric barrier discharge in a tubular cell was investigated. The very steep front voltage ($>10^{12}$ V/s) allowed the reactor to operate at higher reduced field values (E/n) than in conventional DBD systems. To confirm the properties of the non-equilibrium plasma, it was shown that the temperature inside the streamers was around 3,000 K and the mean gas temperature in the active volume was close to room temperature (6).

The effects of CO_2/CH_4 ratio and adding helium to a 1:1 CO_2/CH_4 ratio feed stream were studied. The results indicated that CO_2/CH_4 ratio strongly affected the results. Increasing the partial pressure of carbon dioxide from a 1:2 to 1:1 CO_2/CH_4 ratio caused increased carbon dioxide conversion to carbon monoxide but reduced the ethane and hydrogen selectivities. A further increase in the CO_2/CH_4 ratio from 1:1 to 2:1 caused an increase in ethane and hydrogen selectivities. Despite lowering methane partial pressure, helium acts as a third body in enhancing methane conversion and carbon monoxide selectivities (7).

A numerical simulation was performed to investigate the conversion of methane and carbon dioxide to synthesis gas in a DBD reactor. Using curve-fitting, the H_2/CO ratio can be presented as a simple function of a mixing ratio of CH_4/CO_2 which can be approximated over a wide range. Specific electric energy, gas pressure, and temperature hardly influence syngas composition (2).

The combination of solid catalysts with a dielectric-barrier discharge also has been studied for carbon dioxide reforming of methane. It was shown that the nickel and the nickel-calcium coated foams showed nearly identical activities for the reforming reaction in the discharge in the temperature range of 40 - 230 °C and gave significantly higher carbon monoxide production than the rhodium coated catalyst and the uncoated foam. The reaction was operated over the stoichiometric ratio at a CO_2/CH_4 ratio of 3:1 to minimize hydrocarbon formation. After the reaction, small amount of carbon or carbonaceous deposits were found on the foams (8).

Because the corona discharge is particularly easy to establish, it has had wide application in a variety of processes such as electrostatic precipitation, electro-photography, static control in semiconductor manufacture, ionization instrumentation, destruction of toxic compounds, generation of ozone, and synthesis of chemicals (9).

In this work, a corona discharge reactor was used to facilitate carbon dioxide reforming by itself and in combination with steam at low temperatures. This has been shown to be possible in other methane conversion studies without carbon dioxide, such as helping in the conversion of methane over Sr/La_2O_3 (10) and other materials (11). The disadvantage of using electrical energy, that at best may only be about 60 percent efficient, may be offset by process simplicity and cost, lower carbon formation and less excess energy that must be recovered and utilized only with considerable cost.

6.3 Experimental

The flow rates of feed gases were controlled by a set of mass flow controllers supplied by Porter Instrument, Inc. Water-vapor was introduced into the reactor by passing the feed gases through a water-bath of which the temperature was controlled

to adjust the concentration of water-vapor in the feed gas mixture. The feed gases were well mixed and then flowed downward through the reactor. The reactor temperature was controlled to be constant 100 °C to avoid water condensation during reaction. All the experiments were operated at atmospheric pressure. The feed gases and the exhaust gases from the reactor were introduced into two condensers in series cooled by ice water to remove the condensable products as well as water and then analyzed on-line by a Carle AGC 400 gas chromatograph with thermal conductivity detector. However, no organic products were collected from the condensers when analyzed with a Varian 3300 GC with a Porapak Q Column. The power supply unit consisted of an AC power supply for converting domestic AC power 120 V, 60 Hz, using a function generator to vary the frequency in the range of 300 to 600 Hz with a sinusoidal waveform. The output was then transmitted to a high voltage alternating current (HVAC) transformer. The HVAC transformer could step up the low side voltage to the high side voltage by a nominal factor of 125 at 60 Hz. This factor may not be constant with changes in frequency due to changes in the power factor because of the capacitive nature of the reactor system. The discharge occurred between two stainless steel electrodes in a quartz tube with an inside diameter of 7 mm. The gap distance between these two electrodes was 1 cm. The feed gas flow rate was the same for every experiment at 100 sccm corresponding to a residence time of 0.23 s. The upper wire electrode was centered axially within the reactor tube, while the lower electrode was a circular plate with holes to allow gas to pass through the reactor and positioned perpendicular to the reactor axis. An Extech power analyzer was used to measure the power, power factor, current, frequency, and voltage at the low side of the power circuit.

For this system, the energy consumption for conversion of carbon in the feed gas consisting of methane and carbon dioxide is given in units of electron-volt/molecule of carbon converted (eV/m_C). S_X is defined as the selectivity based on converted carbon in both carbon dioxide and methane. S_{total} is defined as the total selectivities of all products which contain C (carbon atom).

All experiments had a carbon balance greater than 84%. Water was not quantified.



6.4 Results and Discussion

6.4.1 Reaction Pathways in Plasma Environment

The electron energy, which corresponds to the electron temperature, is restricted to less than 6 eV in the corona discharge (12). These relatively low-energy electrons have insufficient energy to ionize methane, which has an ionization potential greater than 12 eV (13), but high enough to dissociate carbon dioxide molecules with dissociation energies of 5.5 eV (Reaction 6.5) (2, 5, 14).



H₂O also requires only a relatively low electron energy to be dissociated to produce O, H and OH radicals as shown in Reactions 6.6 and 6.7 (15):



These radicals, H, OH and O, further abstract hydrogen from methane to form methyl radical (CH₃) leading to a significant rate of methane conversion in the corona discharge (Reactions 6.8-6.10).

Methyl radical formation :



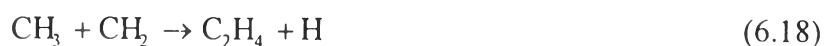
These methyl radicals react further to either combine with another CH₃ to form ethane (Reaction 6.11) or break down into CH₂, CH and C and subsequently form ethylene, acetylene and carbon oxides (16). Ethane can be further dehydrogenated to form ethylene and acetylene and ethylene can be dehydrogenated

to form acetylene. These reaction pathways were also observed in the conversion of methane via microwave plasmas (17). The coupling of hydrogen radicals forms hydrogen. Beyond these main reactions, there may be many contributing reaction pathways in the corona discharge environment. Some of the possible ethane, ethylene, acetylene and hydrogen formation reactions are shown in Reactions 6.11-6.39. Water may be formed in the discharge via Reactions 6.40-6.43.

Ethane formation :

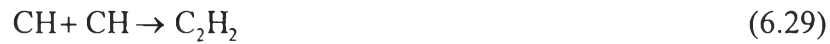


Ethylene formation :

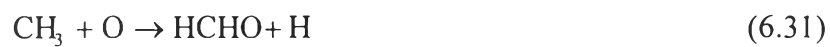


Acetylene formation :





CO_x formation :



Hydrogen formation :



Water formation:



Moreover, the radicals of H, OH, and O generated from dissociation of water are essential ingredient for the inhibition and removal of carbon deposits which have a negative effect on gas discharges, shown in Reactions 6.44 and 6.45 (18).





6.4.2 Effect of Carbon Sources with Water-Vapor

In Table 6.1, the results of a feed stream of 50% methane or carbon dioxide or carbon monoxide reacting with 50% water are shown. Many products, CO, CO₂, C₂H₆, C₂H₄, C₂H₂, and H₂, were produced from methane reacting with water but C₂ products were not produced from carbon dioxide with water or from carbon monoxide with water. Apart from the main reaction of methane reforming with steam in the corona discharge environment, there are also other reactions occurring simultaneously such as hydrogenation, dehydrogenation etc.

The H₂/CO ratio is quite high; more than the stoichiometric ratio for steam reforming. In the industrial catalytic process, the syngas ratio (H₂/CO) obtained with steam reforming is higher than 3 caused by a surplus of steam (19, 20). High hydrogen production here results from the net dehydrogenation with the formation of C₂ hydrocarbon products and hydrogen also can be produced directly from the dissociation of water in the corona discharge as shown in Reaction 6.6. Steam reforming of methane in the low temperature plasma environment is an alternative way to produce synthesis gas instead of the conventional process.

Carbon dioxide with water is essentially unreactive under the conditions of this experiment, where of course both species are strongly favored by thermodynamics. Even though methane with water and carbon dioxide with water have the same current, or an equal the number of electrons to initiate reactions, carbon dioxide conversion is much lower than methane conversion. The products were only oxygen and carbon monoxide with a CO/O₂ ratio of 2.3. Carbon monoxide with water is converted to some extent with the expected production of hydrogen and carbon dioxide. For the CO/H₂O system, the H₂/CO₂ was about 0.9, that is close to the stoichiometric ratio of the water gas shift reaction. Energy consumption of carbon dioxide with water and carbon monoxide with water is very high under these conditions.

Table 6.1 Reactions of methane, carbon dioxide, carbon monoxide with water-vapor.

Carbon (%)	50% CH ₄	50% CO ₂	50% CO
Water-vapor (%)	50	50	50
Low side Voltage (V)	57	85	63
Frequency (Hz)	600	400	600
Power (W)	13	10	7
Power Factor	0.48	0.27	0.49
Current (A)	0.48	0.44	0.23
C conversion (%)	X _{CH₄} = 27	X _{CO₂} = 1	X _{CO} = 6
S _{CO} (%)	35	112	-
S _{CO₂} (%)	1	0	105
S _{C₂H₆} (%)	5	0	0
S _{C₂H₄} (%)	8	0	0
S _{C₂H₂} (%)	39	0	0
S _{total} (%)	88	112	105
Energy consumption (eV/m _C)	14	353	35
H ₂ /CO _x	H ₂ /CO = 4.7	H ₂ /CO = 0.0	H ₂ /CO ₂ = 0.9
CO/C ₂	1.4	-	-
CO/O ₂	-	2.3	-

6.4.3 Effect of Water-Vapor on Carbon Dioxide Reforming with Methane

In Table 6.2, it may be seen that in an excess of carbon dioxide, without water, the methane conversion is low and little carbon dioxide is converted under these conditions. With increasing frequency, keeping power constant at 11 W, the current is nearly constant while the power factor decreased as the low side voltage increased. The power factor decreased with increasing frequency due to the lag between current and voltage waveforms due to the capacitive nature of the reactor system. Frequency affects not only the electrical parameters but also affects conversion and product distribution as well as energy consumption. At these studied conditions, the maximum conversion of methane and carbon dioxide were found at 400 Hz and consequently the lowest power consumption was also found at this

frequency. H_2/CO ratio was constant at 1.3, however, the product distribution changed with frequency. At 400 Hz, CO/C_2 ratio was highest because of decreasing of ethane and ethylene selectivities.

Table 6.2 Carbon dioxide reforming of methane with/without water-vapor at a 3:1 CO_2/CH_4 ratio.

CO_2/CH_4	3	3	3	3
Water-vapor (%)	0	0	0	50
Low side Voltage (V)	57	68	79	82
Frequency (Hz)	300	400	500	400
Power (W)	11	11	11	14
Power Factor	0.56	0.48	0.42	0.39
Current (A)	0.35	0.34	0.33	0.44
CH_4 conversion (%)	12	19	14	53
CO_2 conversion (%)	2	4	2	20
S_{CO} (%)	63	53	48	89
$S_{C_2H_6}$ (%)	14	6	12	0
$S_{C_2H_4}$ (%)	14	9	13	1
$S_{C_2H_2}$ (%)	19	18	15	5
S_{total} (%)	110	86	88	95
Energy consumption (eV/mC)	41	21	33	15
H_2/CO	1.3	1.3	1.3	0.6
CO/C_2	2.7	3.2	2.4	27.5

In the last column of Table 6.2, with addition of water, much higher conversions of both carbon dioxide and methane are achieved. Adding water provides more reactive H, OH, and O radicals in the reaction zone. The reactor could be operated at higher power to obtain higher conversion since these radicals inhibit and remove carbon formation. The net energy consumption (eV/molecule of carbon converted) was lower significantly despite 50 percent dilution of carbon dioxide and methane by the water. In addition, H, OH, and O radicals initiate methyl

radical formation (Reactions 6.8-6.10) resulting in increased methane conversion and decreased energy consumption. H_2 and H produced from dissociation of water (Reactions 6.6-6.7). Little C_2 formation occurs evidently due to dehydrogenation and oxidation of methane such that coupling is inhibited. Most of the C from methane and carbon dioxide form carbon monoxide rather than C_2 products as suggested by the high CO/ C_2 ratio. Simultaneous carbon dioxide and steam reforming produces higher methane conversions and CO/ C_2 ratio than only steam reforming (Table 6.1) or carbon dioxide reforming (Table 6.2).

Oxygen species from decomposition of water has a negative effect on C_2 hydrocarbon formation because the newly formed hydrocarbons are still in excited states and then further to be oxidized with oxygen. In addition, decreasing CH_x concentration with water in the feed stream, makes the coupling of methane less favorable. The H_2/CO ratio drop from 1.3 to 0.6 when the system was operated at 50% of water in the feed stream, even though there is more H atom in the feed gas. The result probably reflects using high power, H from methane and water reform water.

6.4.4 Effect of Power and Water-Vapor on Carbon Dioxide Reforming of Methane with Water-Vapor

At a CO_2/CH_4 ratio of 5:1, methane conversion is substantially increased with a more modest increase in carbon dioxide conversion with increasing power, but there are no significant changes in methane and carbon dioxide conversions with more water content in the feed, as shown in Table 6.3.

With less water, at 30%, the energy consumption per molecule of carbon converted was substantially reduced compared to 50% water. One of the factors is the dilution and therefore lower throughput of methane at the same power level. As previously mentioned, the radicals from the dissociation of water abstract hydrogen from methane to form methyl radicals resulting in increasing methane conversion. However, a greater number of oxygen radicals could speed up the oxidation reaction to produce carbon dioxide, carbon monoxide, and water. For this reason, some input energy is used to convert recovered carbon dioxide so energy consumption per molecule of carbon converted increased with increasing water from

30% to 50%. Also, there is a substantial suppression of C_2 production with increased water content. Consequently, CO/C_2 ratio was very high (~68.8%) at 50% water-vapor in the feed gas. This result is similar to the results in Table 6.2. The H_2/CO ratio is nearly constant at 0.4 over these three conditions

Table 6.3 Effect of power and water-vapor on carbon dioxide reforming of methane with water at a 5:1 CO_2/CH_4 ratio.

CO_2/CH_4	5	5	5
Water-vapor (%)	30	30	50
Low side Voltage (V)	62	75	79
Frequency (Hz)	300	300	400
Power (W)	11	13	14
Power Factor	0.43	0.35	0.43
Current (A)	0.41	0.50	0.41
CH_4 conversion (%)	51	57	58
CO_2 conversion (%)	13	17	18
S_{CO} (%)	85	86	100
$S_{C_2H_6}$ (%)	0	0	0
$S_{C_2H_4}$ (%)	2	2	0
$S_{C_2H_2}$ (%)	13	10	3
S_{total} (%)	100	98	103
Energy consumption (eV/ m_C)	12	12	17
H_2/CO	0.5	0.4	0.4
CO/C_2	11.1	15.0	68.8

6.4.5 Effect of Power and Frequency on Carbon Dioxide Reforming of Methane with Water

The results at the stoichiometric CO_2/CH_4 ratio of 1:1, 50% water-vapor and different frequencies are shown in Table 6.4. Increased power at the 1:1 CO_2/CH_4 ratio shows increased conversion except when the frequency is increased. The increase in frequency essentially “detunes” the system, reducing the power

factor and the power actually applied to the plasma. Power was actually measured on the low voltage side and therefore included all high voltage system losses. The system designed to properly match impedances and operated at a high power could significantly lower the real power consumption from that reported here.

Table 6.4 Effect of power and frequency on carbon dioxide reforming of methane with water at a 1:1 CO₂/CH₄ ratio.

CO ₂ /CH ₄	1	1	1	1
Water-vapor (%)	50	50	50	50
Low side Voltage (V)	57	66	88	97
Frequency (Hz)	300	300	400	600
Power (W)	11	13	14	14
Power Factor	0.54	0.45	0.34	0.40
Current (A)	0.36	0.43	0.47	0.36
CH ₄ conversion (%)	41	44	47	30
CO ₂ conversion (%)	20	21	21	12
S _{CO} (%)	56	60	56	72
S _{C₂H₆} (%)	2	1	1	3
S _{C₂H₄} (%)	5	5	5	5
S _{C₂H₂} (%)	23	24	26	21
S _{total} (%)	86	90	88	101
Energy consumption (eV/m _C)	11	12	12	20
H ₂ /CO	1.9	1.9	1.9	1.7
CO/C ₂	3.9	4.1	3.5	4.9

6.4.6 Effect of CO₂/CH₄ Ratio on Carbon Dioxide Reforming of Methane with Water

Table 6.5 shows the effect of CO₂/CH₄ ratio on carbon dioxide reforming with water. The methane conversion increased with increasing CO₂/CH₄ ratio while carbon dioxide conversion was constant because of the decreasing methane partial pressure. Energy consumption per carbon converted is lower due to

decreased carbon dioxide dilution since methane conversion is the higher of the two. The lower CO_2/CH_4 ratio results in greater C_2 production from the coupling reaction of methane since a decrease in CO_2/CH_4 ratio increases the probability of a methyl radical reacting with another methyl radical. C_2 's may be undesirable components of synthesis gas, but the olefinic nature of those produced here are reactive on Fischer Tropsch catalyst systems and therefore may be suitable for feeds to a Fischer Tropsch Synthesis Reactor. The H_2/CO ratio is close to that desired for Fischer Tropsch or methanol synthesis and may be controllable by altering the water content.

Table 6.5 Effect of CO_2/CH_4 ratio on carbon dioxide reforming of methane with water at 50% water-vapor.

CO_2/CH_4	1	3	5
Water-vapor (%)	50	50	50
Low side Voltage (V)	88	82	79
Frequency (Hz)	400	400	400
Power (W)	14	14	14
Power Factor	0.34	0.39	0.43
Current (A)	0.47	0.44	0.41
CH_4 conversion (%)	47	53	58
CO_2 conversion (%)	21	20	18
S_{CO} (%)	56	89	100
$S_{\text{C}_2\text{H}_6}$ (%)	1	0	0
$S_{\text{C}_2\text{H}_4}$ (%)	5	1	0
$S_{\text{C}_2\text{H}_2}$ (%)	26	5	3
S_{total} (%)	88	95	103
Energy consumption (eV/ m_C)	12	15	17
H_2/CO	1.9	0.6	0.4
CO/C_2	3.5	27.5	68.8

In high temperature catalytic steam reforming of methane, the endothermic heat of reaction must be provided at quite high temperatures with very intense heat fluxes. Although the direct fired furnaces used for this are quite efficient (>90%), they are quite expensive including the cost of heat recovery systems. A plasma discharge reactor system uses electricity to drive the reaction and can be assumed to have an efficiency no greater than that of the power generation system (~60% for modern combined cycle combustion turbine plants). However, for the low temperature plasma, little energy is expended in gas heating and heat recovery systems are not needed. Thus, for the plasma system, somewhat higher energy consumption maybe offset by simple process operation and lower cost for investment. This could be true especially for relatively small scale plants, where fuel gas is inexpensive, or where excess (off peak) power generation is available.

6.5 Conclusions

Carbon dioxide combined with steam reforming at moderate conversion levels has been demonstrated at near ambient conditions with moderate power consumption. Under most conditions, carbon formation was not an operational problem. If long term operation with high conversions can be demonstrated, a process can be envisaged wherein the cost and efficiency of using electricity to drive the reaction is counter-balanced by lower costs and simpler operation (without oxygen). For smaller resources and more remote locations, these tradeoffs may be highly advantageous. Whether there is a net reduction in carbon dioxide impact compared to more conventional reforming/partial oxidation synthesis gas generation processes can only be determined by a detailed life cycle analysis and not simply by the apparent reaction stoichiometry.

6.6 Acknowledgements

ChevronTexaco, Inc. and The Thailand Research Fund are gratefully acknowledged for supporting this research. Helpful discussions with Terence A. Caldwell are also acknowledged.

6.7 References

- 1 Walker, A. V.; King, D. A. *J. Phys. Chem. B* **2000**, 104, 6462-6467.
- 2 Zhou, L. M.; Xue, B.; Kogelschatz, U.; Eliasson, B. *Energy & Fuels* **1998**, 12, 1191-1199.
- 3 Cancino, J. F. Master Thesis, University of Oklahoma, Norman, OK, 2001.
- 4 Mutaf-Yardimci, O.; Saveliev, A. V.; Fridman, A. A.; Kennedy, L. A. *Int. J. Hydrogen Energy* **1998**, 23, 1109-1111.
- 5 Eliasson, B.; Kogelschatz, U.; Xue, B.; Zhou, L.-M. *Ind. Eng. Chem. Res.* **1998**, 37, 3350-3357.
- 6 Motret, O.; Pellerin, S.; Nikravech, M.; Massereau, V.; Pouvesle, J. M. *Plasma Chem. Plasma Proc.* **1997**, 17, 393-407.
- 7 Larkin, D. W.; Leethochawalit, M.; Chavadej, S.; Caldwell, T. A.; Lobban, L. L.; Mallinson, R. G. In *Greenhouse Gas Control Technologies*; Riemer, P.; Eliasson, B.; Wokaun, A.; Eds.; Elsevier Science Ltd.: New York, 1999; pp 397-402.
- 8 Kraus, M.; Eliasson, B.; Kogelschatz, U.; Wokaun, A. *Phys. Chem. Chem. Phys.*, **2001**, 3, 294-300.
- 9 Chang, J.-S.; Lawless, P. A.; Yamamoto, T. *IEEE Trans. Plasma Sci.* **1991**, 19, 1152-1165.
- 10 Marafee, A.; Liu, C.; Xu, G.; Mallinson, R.; Lobban, L. *Ind. Eng. Chem. Res.* **1997**, 36, 632-637.
- 11 Liu, C.; Marafee, A.; Mallinson, R.; Lobban, L. *Appl. Catal. A.* **1997**, 164, 21-33.
- 12 Eliasson, B.; Kogelschatz, U. *IEEE Trans. Plasma Sci.* **1991**, 19, 1063-1077.
Sorensen, S. L.; Karawajczyk, A.; Stromholm, C.; Kirm, M. *Chem. Phys. Lett.* **1995**, 232, 554-560.
- 13 Eliasson, B.; Liu, C.-J.; Kogelschatz, U. *Ind. Eng. Chem. Res.* **2000**, 39, 1221-1227.
- 14 Liu, C.; Marafee, A.; Hill, B.; Xu, G.; Mallinson, R.; Lobban, L. *Ind. Eng. Chem. Res.* **1996**, 35, 3295-3301.

- 15 Huang, A.; Xia, G.; Wang, J.; Suib, S. L.; Hayashi, Y.; Matsumoto, H. *J. Catal.* **2000**, *189*, 349-359.
- 16 Suib, S. L.; Zerger, R. P. *J. Catal.* **1993**, *139*, 383-391.
- 17 Liu, C.-J.; Mallinson, R.; Lobban, L. *J. Catal.* **1998**, *179*, 326-334.
- 18 Tjatjopoulos, G. J.; Vasalos, I. A. *Ind. Eng. Chem. Res.* **1998**, *37*, 1410-1421.
- 19 Kraus, M. Ph.D. Thesis, TU Karlsruhe, Germany, 2001.